In Situ Trace Analysis of Oil in Water with Mid-Infrared Fiberoptic Chemical Sensors

ARTICLE *in* ANALYTICAL CHEMISTRY · NOVEMBER 2011

Impact Factor: 5.64 · DOI: 10.1021/ac201664p · Source: PubMed

4 AUTHORS, INCLUDING:

Bogdan Zdyrko
Clemson University
57 PUBLICATIONS **1,741** CITATIONS
SEE PROFILE

Boris Mizaikoff
Universität Ulm
311 PUBLICATIONS **4,809** CITATIONS
SEE PROFILE

analytical chemistry

ARTICLE

pubs.acs.org/ac

In Situ Trace Analysis of Oil in Water with Mid-Infrared Fiberoptic Chemical Sensors

Yuliya Luzinova,[†] Bogdan Zdyrko,[‡] Igor Luzinov,[‡] and Boris Mizaikoff*[,§]

[†]School of Chemistry and Biochemistry, Georgia Institute of Technology, Atlanta, Georgia 30332-0400, United States

[‡]School of Material Science and Engineering, Clemson University, Clemson, South Carolina 29634, United States

[§]Institute of Analytical and Bioanalytical Chemistry, University of Ulm, 89081 Ulm, Germany

Supporting Information

ABSTRACT: The determination of trace amounts of oil in water facilitates the forensic analysis on the presence and origin of oil in the aqueous environment. To this end, the present study focuses on direct sensing schemes for quantifying trace amounts of oil in water using mid-infrared (MIR) evanescent field absorption spectroscopy via fiberoptic chemical sensors. MIR transparent silver halide fibers were utilized as optical transducer for interrogating oil-in-water emulsions via the evanescent field emanating from the waveguide surface, and penetrating the surrounding aqueous environment by a couple of micrometers. Unmodified fibers and fibers surface-modified with grafted epoxidized polybutadiene layers enabled the direct detection of crude oil in a deionized water matrix at the ppm level to ppb concentration level, respectively. Thus, direct chemical sensing of crude oil IR signatures without any sample preparation as low as 46 ppb was achieved with a response time of a few seconds.

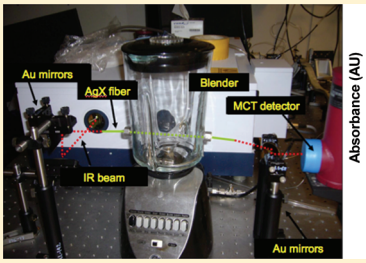

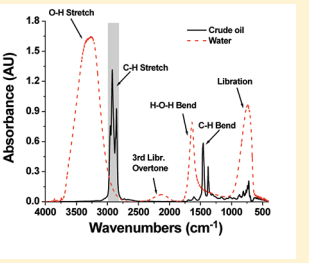

INTRODUCTION

Oil spills occur every day worldwide, and the large spills may cause extensive damage to marine life, terrestrial life, human health, and natural resources.[1−5] Oil that enters the ocean comes from many sources, some being natural seepage,[3] and some being accidental spills or leaks.[1,4,6] Therefore, the impact of oil contamination on the surrounding ecosystems and its long-term effects are major global concerns.[5] As a result, the detection of trace amounts of oil in water is important for monitoring our ecosystems and natural habitats.[7] This novel technique also may assist in discovering new oil deposits.

In recent years, the detection of hydrocarbons in water has successfully been advanced, however, based on methods that usually operate ex situ and off-line, and require comparatively sophisticated sample preparation strategies at extended analysis times.[8−10] UV spectroscopy based systems for in situ analysis have matured to a device technology that is currently already implemented at oil rigs.[11,12] Alternative analytical techniques including infrared (IR) spectroscopy represent a viable alternative for providing rapid screening results without or with minimal sample preparation.[13−15] Today, a number of portable IR analytical systems based on single-reflection diamond waveguides and/or multireflection horizontal attenuated total reflection (ATR) devices have been reported.[2,13,14]

Sensors utilizing IR-ATR evanescent field absorption spectroscopy as the fundamental measurement principle inherently provide the capability of evaluating both viscous and highly absorbing samples in aqueous environments.[13,16−18] Alternatively, portable systems using fiberoptic probes with a sensing tip have been operated in reflection mode for direct analysis,[2] as well as mid-infrared (MIR) spectroscopy coupled with multivariate pattern recognition methods for characterizing oil pollutions.[19−22] Moreover, a variety of portable hand-held MIR analyzers have been reported in the past few years.[23,24]

Despite the significant number of reported MIR sensing techniques, the limits of detection and the sensitivity have to date not been comparable to gas chromatography coupled with mass spectrometry (GC-MS) techniques for analyzing trace amounts of oil in water.[1,10] Useful limits of detection for IR based methods have only been reported for using separation techniques or solvent extractions prior to the spectroscopic analysis, which significantly increases the analysis time, and renders these strategies less useful for in situ analysis.[13,14,25−34]

Therefore, it is of importance to develop straightforward to use, sensitive, cost-effective, rapid, and miniaturizable techniques for on-site and in situ analysis of crude oil traces in water. The present study reports on the design and testing of a highly sensitive MIR evanescent field fiberoptic sensor system for the detection of crude oil in water. Polymer or polymer-like films have already been deposited onto waveguide surfaces for enhancing the detectivity of various target constituents.[35−38] For achieving the required sensitivity and limit of detection in crude oil analysis, the fiberoptic waveguide was coated with a hydrophobic polymer membrane (epoxidized polybutadiene, EPB),

Received: August 15, 2011
Accepted: November 21, 2011
Published: November 21, 2011

which attracts hydrophobic crude oil traces to the transducer surface, and within the penetration depth of the evanescent field. It is shown that direct MIR sensing technique detects down to 46 ppb of crude oil in a deionized (DI) water matrix. To the best of our knowledge, this is the smallest amount of crude oil detected to date using MIR sensing technique without prior separation, solvent extraction, or sample preparation of any kind.

EXPERIMENTAL SECTION

An expanded experimental section can be found in the Supporting Information (SI), Section 1.

Reagents and Sample Preparation. Natural crude oil supplied by ExxonMobil Research and Engineering Company (Annadale, NJ) was added to DI water (R = 18.2 MΩ cm at 25 °C) for the preparation of oil-in-water sample. Polybutadiene [M_w = 424 540 g/mol, PDI 2.93 (GPC)] from Aldrich was epoxidized in $CHCl_3$ solution in the presence of stoichiometric (to double bonds) amounts of formic acid, and 30% hydrogen peroxide.[39]

EPB Layer Deposition. The IR-transparent fiber, bare core silver halide fibers (AgX, X = $Cl_{0.3-0.4}Br_{0.7-0.6}$) purchased from JT Ingram Technologies Inc., was coated with EPB by a dip-coating procedure using a DC Mono 160 dip-coater (NIMA Technologies Ltd.). The same experiment was performed at the surface of a silicon wafer (Semiconductor Processing Co.) for determining the thickness and swellability of the grafted EPB layer via ellipsometry. The morphology of the EPB film was furthermore imaged with atomic force microscopy (AFM). All experiments during the present study were performed using the same EPB-coated fiber, thus providing a first indication on the potential robustness of this sensing concept. For the removal of crude oil from the EPB-coated fiber, the transducer was rinsed first with hexane and then with acetone after each experiment to remove any residual water without any measurable degradation of the membrane properties.

Instrumentation and Characterization. The stirring cell setup for studying traces of oil in water was designed around a Bruker Equinox 55 Fourier transform (FT-IR) spectrometer (Bruker Optics Inc., Billerica, MA). The stirring cell was based on a commercial kitchen blender with a volume of approximately 1000 mL, which was adapted for enabling the preparation of oil-in-water emulsions, and for IR spectroscopically analyzing the oil-in-water matrix. For spectroscopic access a 45 cm long bare core silver halide (AgX) fiber segment with a diameter of 700 μm was inserted through the liquid phase contained within the blender with a length of 15 cm exposed to the aqueous matrix (details on the optical setup are described in SI, section 1). The detected signal was processed via an impedance-matched MCT-1000 preamplifier (Infrared Associates, Stuart, FL) (experimental setup is displayed in SI, Figure S-2).

Ellipsometry was performed with a COMPEL automatic ellipsometer (InOmTech, Inc.). AFM studies were conducted using a Dimension 3100 (Digital Instruments, Inc.). Static contact angle measurements were collected using a contact angle goniometer (Kruss, model DSA10).

Spectral Data Analysis. Each experiment was performed three times using the same AgX fiberoptic waveguide. During the reported experiments, each sample concentration was recorded five times averaging 250 scans per spectrum in measurement intervals of 80 s at a spectral resolution of 2 cm^{-1}. The fifth spectrum of each series was evaluated via peak area (PA) integration. Thus, each concentration was evaluated within a total measurement period of approximately 6 min. However, already after the second or third recorded spectrum (i.e., after approximately 3−4 min of measurement time) usually a stable signal representing the crude oil concentration in water was obtained.

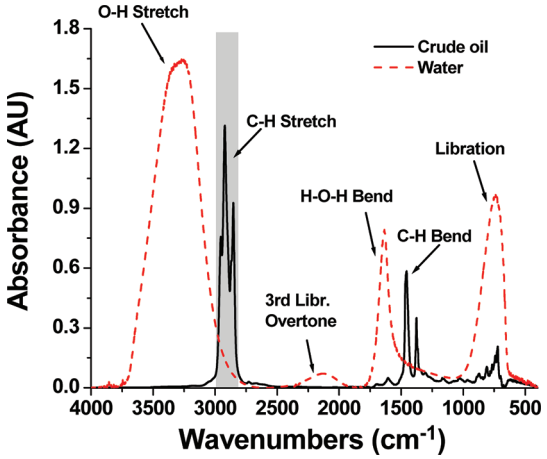

Figure 1. Overlay of the IR-ATR spectra of DI water and crude oil.

Using the OPUS software package (Bruker Optics Inc., Billerica, MA), characteristic infrared absorption features of crude oil were evaluated by peak area analysis; the peak areas associated with the CH stretch absorption at 2940−2880 cm^{-1} were integrated. Figure 1 shows the spectral regions of interest utilized for data analysis in representative IR-ATR spectra of crude oil in water. Peak areas from each spectral region collected during replicated measurements were averaged prior to any further calculations. Consequently, from here on the three averaged peak areas for a given spectral region and the respective sample mixture will be indicated as PA.

RESULTS AND DISCUSSION

As the present study is focused on quantifying trace amounts of oil in water via IR fiberoptic evanescent field absorption spectroscopy, a real world measurement scenario was simulated by emulsifying oil in a DI water matrix with the optical transducer immersed into that mixture. Emulsion conditions were sustained by taking advantage of a stirring cell based on a conventional kitchen blender ensuring continuous turbulent stirring of the oil-in-water sample. This emulsion was created without any addition of surfactant, and is representative for a macroemulsion with a droplet size of a few micrometers.[40] Specifically, it was shown that the size of the oil droplets at these conditions is on the order of 10−100 μm.[41−44] Initial studies have revealed that this experimental setup enables monitoring the molecular constituents within the mixture generated in the stirring cell (Figure 1). Crude oil is characterized by pronounced signatures at 2940−2880 cm^{-1} (CH stretching vibrations), and 1500−1350 cm^{-1} (CH bending vibrations).[27] In this study, the CH stretch region has been selected for quantitative evaluations, as it provides the most pronounced signatures. The CH stretching vibrations overlap with with the OH stretching absorption of water (3750−2750 cm^{-1})[45] (Figure 1). However, the CH stretch is clearly detectable at the shoulder of the OH stretch, thus rendering the detection of crude oil in water straightforward.

dx.doi.org/10.1021/ac201664p |Anal. Chem. 2012, 84, 1274–1280

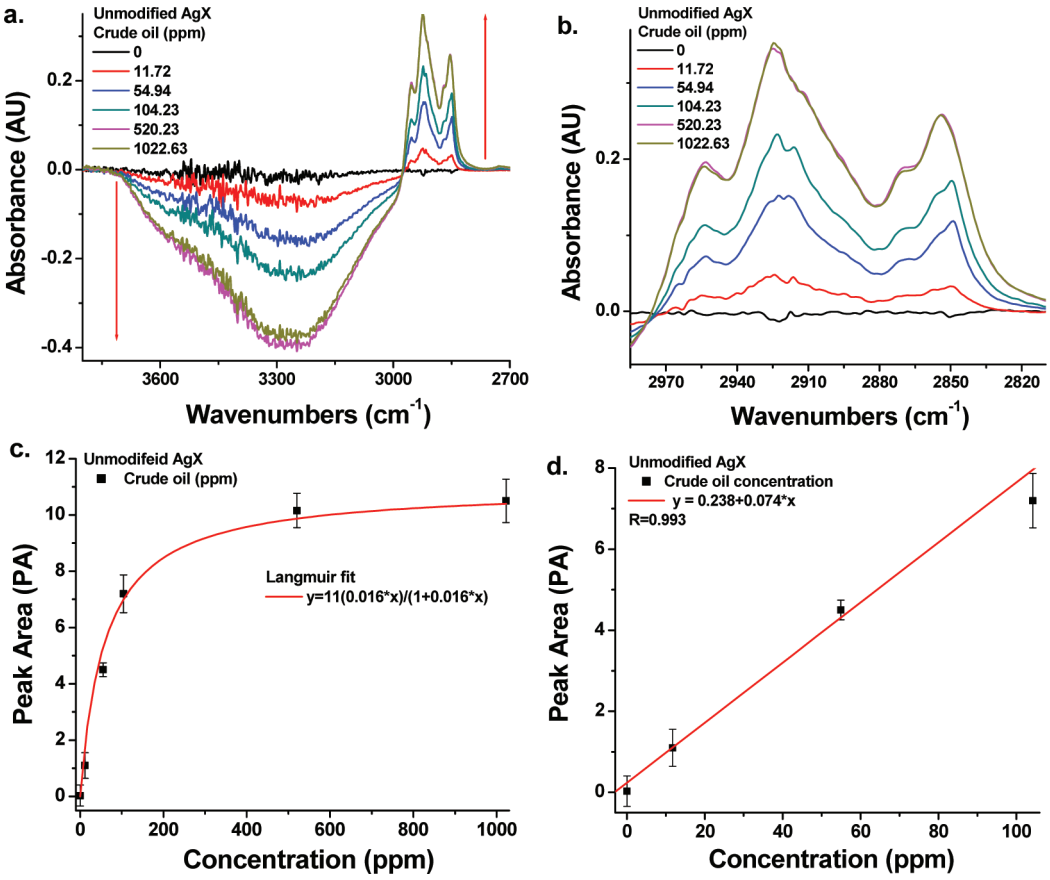

Figure 2. Unmodified fiber: (a) IR spectra of crude oil content in DI water as oil concentration increases from 0 to 1023 ppm, (b) enlarged region of CH stretch of crude oil, (c) Langmuir-type fit, (d) first order linear calibration curve.

Unmodified Fiber. First, experiments using unmodified AgX fibers were performed for evaluating how an increase of crude oil content in DI water affects the IR signature of the emulsion. Hence, crude oil was added into the constantly stirred aqueous environment at a concentration of 0−1023 ppm, and IR spectra were continuously acquired. It should be noted that it was confirmed that the size of the oil droplets does not vary at such low oil concentrations, if the stirring parameters were kept constant.[44] Therefore, changes in the IR spectra, as concentration of oil is increased, are not convoluted with effects resulting from a change in the diameter of the oil droplets.

Figure 2a presents IR spectra of oil in DI water, as the oil concentration increases from 0 to 1023 ppm. As illustrated by the arrows in Figure 2a, the absorbance intensity of the CH stretch increases as the crude oil concentration increases, and the absorbance intensity of the OH stretch associated with water correspondingly decreases. The obtained result demonstrates that evidently crude oil displaces water from the analytical volume probed by the evanescent field adjacent to the waveguide surface. Visual inspection has confirmed that oil is indeed present at the fiber surface. Once the oil content in the system is increased beyond 520 ppm, the absorbance intensity remains constant (Figure 2b). These results indicate that at such relatively high concentrations additional oil may not be detected by the fiberoptic transducer, as the waveguide surface is evidently fully covered with crude oil. In fact, it may be estimated that the absorbance intensity does not further increase from approximately 280 ppm of oil in water onward (Figure 2c).

The peak area of each CH absorption feature was integrated during three parallel measurements for establishing a calibration function to correlate absorbance versus concentration of crude oil in water from 0 to 1023 ppm. The fit parameters for establishing calibration functions are summarized in SI, Table S-1. The plot in Figure 2c may be described by Langmuir-type equation surface coverage[46] (refer to SI section 3, eq S-1). The calibration curve indicates that it is possible to differentiate between the absence of oil in DI water and approximately 12 ppm. At concentrations below 12 ppm, no evaluable IR signature of oil was established. The LOD and LOQ derived from the Langmuir-type fit were calculated to be 7 and 16 ppm, respectively (Table S-1, the criteria for calculating LOD and LOQ can be found in SI secion 1).

In addition, Figure 2c shows that concentrations from 0 to 104 ppm follow a linear trend; thus, a first order linear calibration curve was established for this concentration range (Figure 2d). The goodness of the fit (R value) of 0.99 clearly confirms the linear trend. Using the linear calibration function, the LOD and LOQ were determined to be 12 and 27 ppm, respectively, which are similar to the ones derived from the Langmuir-type fit (Table S-1).

As indicated above, the IR signatures obtained from oil are associated with the deposition of oil droplets attracted to the fiber surface (the diagram of this phenomenon is presented in SI, Figure S-4). Once a droplet is present at the fiber surface, two possible scenarios may occur.

Table 1. Surface Energies and Contact Angles for Liquids and Substrates

substance	γ, mJ/m^2	γ^d, mJ/m^2	γ^p, mJ/m^2	contact angle, deg: DI water	contact angle, deg: hexadecane
unmodified fiber	46.1	27.25	19.8	58	5
EPB film	32.74	26.25	6.5	81	5
water[a]	72.8	21.8	51	N/A	N/A
oil (hexadecane)[a]	26.35	26.35	0	N/A	N/A

[a] From ref 54.

Table 2. Thermodynamic Parameters for Oil/Water/Fiber System

parameter[a]	unmodified fiber	fiber modified with EPB
γ_{12},[b] mJ/m	14.2	34.9
γ_{32},[b] mJ/m	51.4	51.4
γ_{13},[b] mJ/m	19.8	6.5
λ_{31},[b] mJ/m	−57.1	−21
contact angle,[b] deg	96	56.5
W_A,[b] mJ/m	45.8	79.8

[a] Hexadecane was used in calculations as an oil surrogate. [b] Contact angle is calculated for oil (hexadecane) on fiber in water matrix.

In the first scenario, it is assumed that the droplet spreads across the fiber surface to maximize its contact area. The tendency of a material to spread across a surface within a matrix of another material is described via the spreading coefficient[47,48]

$$\lambda_{31} = \gamma_{12} - \gamma_{32} - \gamma_{13} \quad (1)$$

where γ_{12}, γ_{32}, and γ_{13} are the interfacial energies (tensions) for each component pair. Here, λ_{31} is defined as the spreading coefficient for oil (component 3) at the fiber surface (component 1). The index 2 refers to the water matrix. λ_{31} must be positive for 3 (oil) to spread across 1 (fiber) in the presence of matrix 2 (water). If λ_{31} is negative, the second possible scenario is in effect.

In the second scenario, the droplet of oil in contact with the fiber surface will exhibit a certain value for the contact angle (θ), which may be estimated via the following equation:[49]

$$\cos\theta = \frac{\gamma_{12} - \gamma_{13}}{\gamma_{32}} \quad (2)$$

The spreading of oil across the fiber should provide the highest sensitivity for IR evanescent field sensing, as more material is located within the penetration depth of the evanescence field extending a couple of hundred nanometers from fiber surface in the wavelength regime of interest.[17] Consequently, the highest sensitivity of oil for the contact angle scenario will depend on the value of the contact angle. Indeed, from straightforward geometrical considerations it is evident that at lower values of the contact angle more oil from the droplet will be located within the evanescence field (refer to SI, Figure S-4).

In order to differentiate between both scenarios, the interfacial energies for each component pair was estimated from the following equation[50]

$$\gamma_{ab} = \gamma_a + \gamma_b - \frac{4\gamma_a^d \cdot \gamma_b^d}{\gamma_a^d + \gamma_b^d} - \frac{4\gamma_a^p \cdot \gamma_b^p}{\gamma_a^p + \gamma_b^p} \quad (3)$$

where subscripts a and b represent components, and superscripts d and p refer to the dispersive and polar contributions to the surface energy γ, respectively. The dispersive and polar contributions to the surface energy may be obtained from contact angle measurements using the following expressions[51]

$$\gamma = \gamma^d + \gamma^p \quad (4)$$

$$1 + \cos\theta \approx 2\left[\frac{(\gamma_S^d)^{0.5}(\gamma_L^d)^{0.5}}{\gamma_L} + \frac{(\gamma_S^p)^{0.5}(\gamma_L^p)^{0.5}}{\gamma_L}\right] \quad (5)$$

where γ_S^d, γ_S^p, and γ_L^d, γ_L^p, are dispersive and polar components for the surface energy of solid (γ_S) and liquid (γ_L), respectively. These equations permit the derivation of γ_S, γ_S^d, and γ_S^p via measurements of the contact angles of two liquids, if γ_L, γ_L^p, and γ_L^d for both liquids are known.

During the present study, the contact angles at the fiber surface for water and hexadecane have been determined, and the spreading coefficient and contact angle for the oil/water/fiber system have been estimated (Table 1 and 2). Hexadecane has been used as model for oil in these estimations. The thermodynamics indicate ($\lambda_{31} < 0$) that there is no spreading of oil across the fiber in the water matrix. Conversely, a relatively high contact angle (96°) is formed, if an oil droplet is in contact with the unmodified fiber surface. Therefore, a measurable increase in sensitivity and improvement of the limit of detection for crude oil in water is subject to an appropriate chemical modification of the fiber surface tailored to the detection of crude oil.

Surface-Modified Fiber. In order to appropriately modify the fiber surface, a thin layer of epoxidized polybutadiene was deposited via dip coating from chloroform solution followed by annealing. A similar layer was deposited from the same stock solution onto the surface of a silicon wafer. Ellipsometry performed at the film deposited at the wafer surface has indicated that a film thickness of approximately 45 nm was obtained.

The selection of EPB was predominantly based on the relative hydrophobicity of the polymer. In fact, the water contact angle for an EPB film deposited at the model silicon wafer substrate is approximately 81°, which is significantly higher than the water contact angle of 58° determined at the unmodified fiber surface (Table 1). Thermodynamic calculations (using eqs 1−5, Table 2) revealed that the surface modification of the fiber with the hydrophobic polymer does not cause spreading of the oil across the modified fiber in the water matrix ($\lambda_{31} < 0$). However, the contact angle of oil at the fiber for the oil/water/fiber system decreases significantly from 96° to 56.5° (Table 2 and Figure S-4, right and left, respectively). Thus, the amount of oil contributing to the IR signal increases, as a higher fraction per adherent 10−100 μm droplet is absorbing within the evanescent field.

Another reason for selecting EPB is based on the reactivity of the epoxy functionalities of the polymer, which ensure excellent adhesion between the EPB coating and the fiber surface.[52] Additionally, the epoxy groups may react with each other at higher temperatures, which results in cross-linking of the deposited layer thus preventing delamination. In fact, it was shown that EPB-modified fibers and wafers may be rinsed with chloroform, which is an exellent solvent for EPB, several times without removal of the layer.

The EPB films deposited at the silicon wafer surface and at the AgX fiber were thoroughly characterized. AFM images of the unmodified fiber and silicon wafer along with EPB-modified

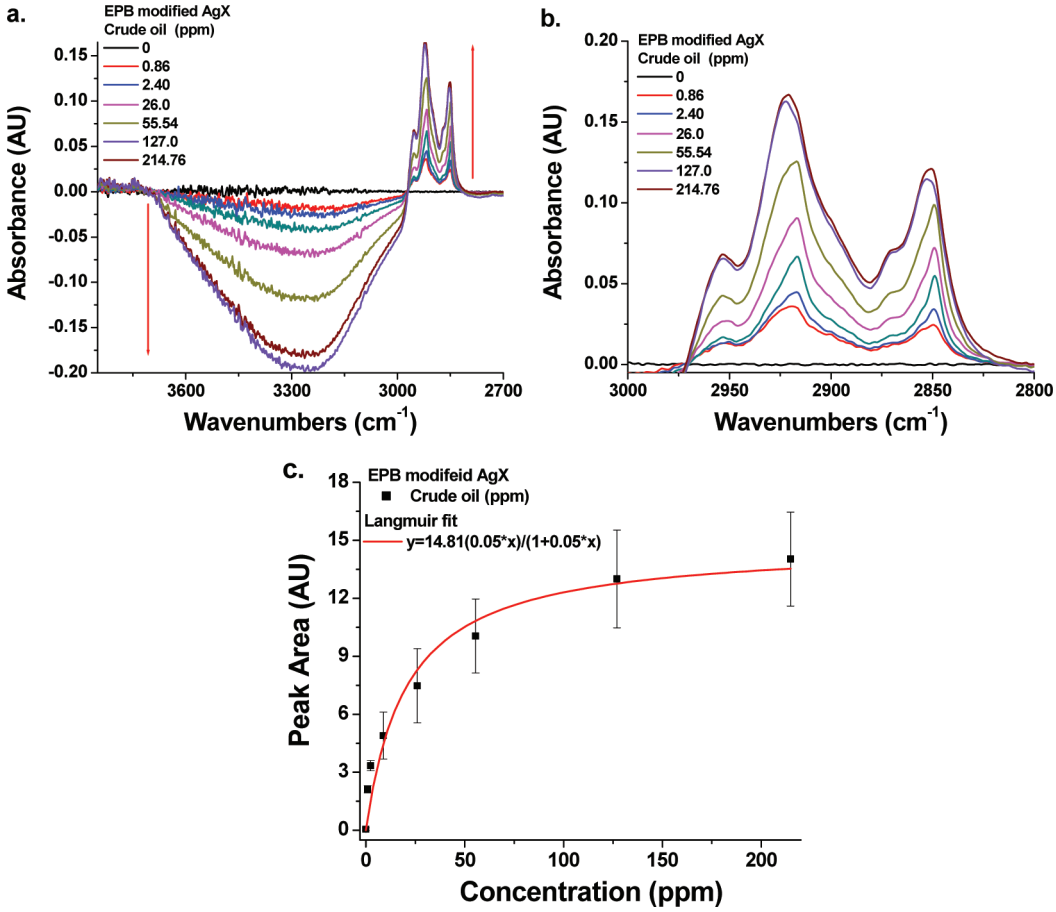

Figure 3. Modified with EPB layer fiber: (a) IR spectra of crude oil content in DI water as oil concentration increases from 0 to 215 ppm, (b) enlarged region of CH stretch of crude oil, (c) Langmuir-type fit.

substrates are presented in SI, Figure S-5. AFM imaging after the substrate (wafer) was covered with the EPB layer and exposed to stirring water, and (in a separate experiment) to hexadecane for approximately 3 h, did not reveal any significant changes in surface morphology. Additionally, ellipsometry measurements revealed no removal of the polymer layer after water and hexadecane contact.

Finally, the level of interaction of hydrocarbons and water with the EPB layer was studied via ellipsometric measurements investigating the swelling behavior of the film in the presence of water and hexane vapors. During these experiments, the EPB layer demonstrated somewhat higher affinity to hexane (6% swelling) than to water (2% swelling). However, if for comparison the layer was exposed to the vapor of a solvent such as chloroform, the thickness of the EPB film was increased by more than 80%. In summary, the swellability studies have demonstrated that only minute amounts of oil and water are evidently absorbed by the EPB layer during IR measurements of the oil content in an oil/water emulsion.

Figure 3a,b shows IR spectra of oil emulsions in DI water, as the oil concentration is increased from 0 to 215 ppm. The spectroscopic data demonstrate that the absorbance intensity of the CH stretch increases, as the crude oil concentration increases. Simultaneously, the peak at 3750−2750 cm^{-1} associated with water decreases. These results indicate that oil displaces water at the fiber surface. Once the oil concentration reaches approximately 110 ppm, the signal associated with oil does not increase any further, thereby indicating that the fiber is covered with crude oil wihin the evanescent field. This value is approximately 2.5 times lower that the saturation value of approximately 280 ppm obtained for the unmodified fiber (Figures 2c and 3c). This observation is directly related to the contact angle between oil droplets and the fiber surface in the oil/water/fiber system. In fact, it may be estimated (see SI, Section 2) that the contact area for an oil drop increases approximately 2-fold, if the contact angle decreases from 96° (unmodified fiber) to 56.5° (EPB modified fiber).

Figure 3c illustrates the PA of the CH stretching vibration versus the concentration of crude oil. Additionally, a Langmuir-type curve (eq S-1) was fitted to the calibration points in Figure 3c. It is evident from Figure 3a−c that it is possible to detect oil in DI water concentrations <1 ppm.

The IR absorption signal associated with an oil concentration of 1 ppm is relatively strong (Figure 3a); thus, measurements at lower concentrations were performed at ppb levels of oil in water. Figure 4a presents IR spectra of oil content in water as the oil concentration increases from 0 to 1 ppm. Figure 4b illustrates a Langmuir-type fit (eq S-1) for the PA versus crude oil concentrations. (Fitting parameters are given in SI, Table S-1.) The higher effective equilibrium constant (K) values (refer to SI, Langmuir-type fit eq. S-1) were obtained for the lower concentrations of oil in water rather than for the higher concentrations, which is explained as follows. At low concentrations the probability that the droplet arriving to the surface will land on the

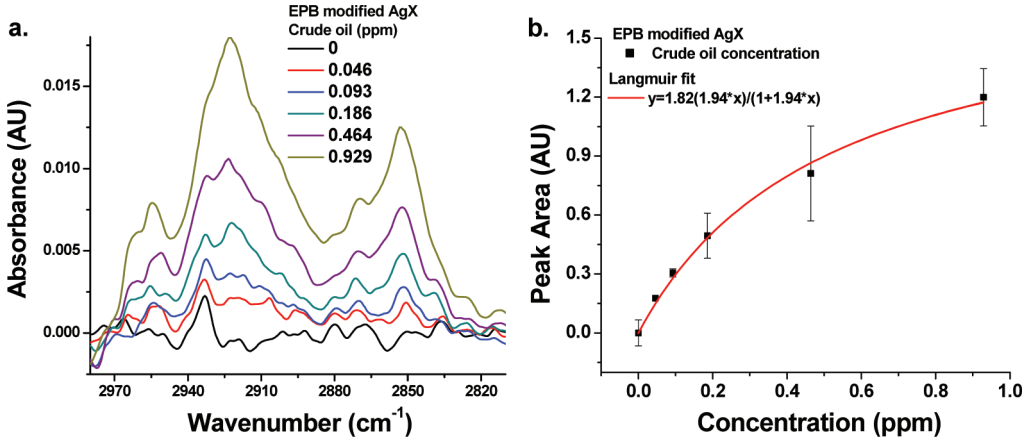

Figure 4. (a) IR spectra of CH stretch of crude oil content in DI water as oil concentration increases from 0 to 1 ppm, and (b) Langmuir-type fit.

droplet which is already located on the fiber is low. Therefore, practically each arriving droplet contributes to the IR signal until a certain point. This leads to the nonlinearity of the overall oil detection process, different and higher K values.

The data presented in Figure 4b indicate that it is possible to still differentiate between 0 ppb oil in water and 46 ppb. Thus, the threshold sensitivity of this experimental setup utilizing EPB-modified AgX fibers is 46 ppb of oil in DI water. Calculated LODs and LOQs for the established calibration curve were determined at 63 and 140 ppb, respectively (Table S-1). It is anticipated that further optimization of the experimental setup in terms of optical robustness will further improve LODs and LOQs.

The obtained results impressively demonstrate that an appropriate surface modification of the transducing fiber directly and positively affects the LOD and LOQ by decreasing the figures-of-merit from approximately 12 and 27 ppm to 63 and 140 ppb, respectively (Table S-1). Thus, with AgX EPB-modified waveguides the obtained LOD and LOQ were almost 200-times better than for unmodified transducers. Even visually analyzing the IR spectra of crude oil in DI water using polymer modified fibers enabled the identification of approximately 46 ppb compared to approximately 12 000 ppb at unmodified fibers.

Besides the difference in oil-fiber contact, the significantly improved performance of the coated fiber may be further explained by enhanced adhesion between oil droplets and the fiber surface at EPB-modified fibers. The level of adhesion may be approximated via the work of adhesion (W_A) defined as the reversible work required to separate a unit area of liquid from a substrate.[48,53] In the case of oil/water/fiber system considered in the present study, the work of adhesion is defined as

$$W_A = \gamma_{12} + \gamma_{32} - \gamma_{13} \quad (6)$$

The higher the value of W_A, the stronger the adhesion between the oil droplet and the fiber surface. Calculations of W_A for the modified and unmodified fibers are reported in Table 2. The work of adhesion is approximately 2 times higher for the fiber modified with the EPB layer. Additionally, taking into account the increase in surface contact area between oil droplets and the AgX fiber surface, which is approximately 2-fold for the EPB-modified fiber, the work of adhesion per droplet becomes approximately 3.5 times higher for EPB-modified AgX fibers. Therefore, in a constantly stirred water matrix resembling continuous movement of a real-world sample, the probability of attachment of an oil droplet to the fiber surface (thus contributing to the analytical signal) is significantly higher for the surface-modified fiber. Analogously, the probability of detachment of the already attached droplet is lower for the coated fiber.

CONCLUSIONS

In this study, MIR evanescent field absorption spectroscopy based on a fiberoptic chemical sensor was applied to detect and quantify trace amounts of crude oil in oil/water emulsions without prior sample separation or solvent extraction. Unmodified fibers enabled detecting the presence of crude oil in a DI water matrix at approximately 12 ppm concentration levels. A chemical surface modification of the silver halide waveguide via an epoxidized polybutadiene (EPB) polymer layer has enabled the direct in situ detection of crude oil IR signatures in DI water at low ppb concentration levels of approximately 46 ppb. The obtained results during thorough characterization of the EPB layer indicate that the enhanced performance of the surface-modified fiber is associated with the increased oil/fiber wettability, and adhesive forces of oil at the EPB-modified transducer surface. To the best of our knowledge, the proposed IR-based sensing technique uniquely enables directly detecting such low oil concentrations in aqueous environments.

ASSOCIATED CONTENT

Supporting Information. Expanded experimental section, details on the method for the determination of the contact area for droplets deposited at the fiber surface, and supporting tables, figures, and equations. This material is available free of charge via the Internet at http://pubs.acs.org.

AUTHOR INFORMATION

Corresponding Author

*E-mail: boris.mizaikoff@uni-ulm.de.

ACKNOWLEDGMENT

The authors would like to thank Bruker Optics (Billerica, MA, and Ettlingen, Germany) for generous instrumental support. The authors are grateful for funding, scientific support, and discussions provided by Exxon Mobil Research and Engineering Company (EMRE). Special thanks are extended to

Dr. Mark M. Disko, Dr. John Szobota, and Dr. Clifford Walters for the excellent collaboration, numerous scientific discussions, and advice during this study. B.Z. and I.L. acknowledge the DoE NA-22 program (Contract DE-NA000421) for partial support of this work. Therefore, this paper has been prepared as an account of work partially supported by an agency of the United States Government. Neither the United States Government nor any agency thereof, nor any of their employees, makes any warranty, express or implied, or assumes any legal liability or responsibility for the accuracy, completeness, or usefulness of any information, apparatus, product, or process disclosed, or represents that its use would not infringe privately owned rights. Reference herein to any specific commercial product, process, or service by trade name, trademark, manufacturer, or otherwise does not necessarily constitute or imply its endorsement, recommendation, or favoring by the United States Government or any agency thereof. The views and opinions of authors expressed herein do not necessarily state or reflect those of the United States Government or any agency thereof.

REFERENCES

(1) Wang, Z. D.; Fingas, M. F. *Mar. Pollut. Bull.* **2003**, *47*, 423–452.
(2) Perez-Caballero, G.; Andrade, J. M.; Muniategui, S.; Prada, D. *Anal. Bioanal. Chem.* **2009**, *395*, 2335–2347.
(3) National Research Council. *Oil in the Sea III: Inputs, F., and Effects III*; National Academies Press: Washington, DC, 2003; p 192; http://www.nap.edu/openbook.php?record_id=10388&page=191.
(4) Tanobe, V. O. A.; Sydenstricker, T. H. D.; Amico, S. C.; Vargas, J. V. C.; Zawadzki, S. F. *J. Appl. Polym. Sci.* **2009**, *111*, 1842–1849.
(5) Fingas, M. F.; Brown, C. E. *Spill Sci. Technol. Bull.* **1997**, *4*, 199–208.
(6) *Oil Spill Intelligence Report's White Paper Series*; Etkin, D. S., Ed.; Cutter Information Corp.: Arlington, MA, 1998.
(7) Begak, O. Y.; Syroezhko, A. M. *Russ. J. Appl. Chem.* **2001**, *74*, 636–639.
(8) Stenstrom, M. K.; Fam, S.; Silverman, G. S. *Environ. Technol. Lett.* **1986**, *7*, 625–636.
(9) Nemirovskaya, I. A.; Anikiev, V. V.; Theobald, N.; Rave, A. *J. Anal. Chem.* **1997**, *52*, 349–353.
(10) Wang, Z. D.; Fingas, M. *J. Chromatogr., A* **1997**, *774*, 51–78.
(11) SL Ross Environmental Research. http://www.boemre.gov/tarprojects/598/smartcotsproductsreportfinal.pdf (accessed on 10/19/2011).
(12) www.oilinwatermonitors.com (accessed on 10/19/2011).
(13) http://www.wilksir.com/ (accessed on 10/19/2011).
(14) Minty, B.; Ramsey, E. D.; Davies, I. *Analyst* **2000**, *125*, 2356–2363.
(15) *ASTM D7575: Standard Test Method for Solvent-Free Membrane Recoverable Oil and Grease by Infrared Determination*; ASTM International Standards.
(16) Mizaikoff, B. *Meas. Sci. Technol.* **1999**, *10*, 1185–1194.
(17) Mizaikoff, B. *Anal. Chem.* **2003**, *75*, 258A–267A.
(18) Mizaikoff, B.; Jakusch, M.; Kraft, M. *Sea Technol.* **1999**, *40*, 25.
(19) Fernandez-Varela, R.; Andrade, J. M.; Muniategui, S.; Prada, D.; Ramirez-Villalobos, F. *Mar. Pollut. Bull.* **2008**, *56*, 335–347.
(20) Fresco-Rivera, P.; Fernandez-Varela, R.; Gomez-Carracedo, M. P.; Ramirez-Villalobos, F.; Prada, D.; Muniategui, S.; Andrade, J. M. *Talanta* **2007**, *74*, 163–175.
(21) Staniloac, D.; Petrescu, B.; Patroeseu, C. *Environ. Forensics* **2001**, *2*, 363–366.
(22) Ruyken, M. M. A.; Pijpers, F. W. *Anal. Chim. Acta* **1987**, *194*, 25–35.
(23) Rotteri, S.; H. B., Dubreuil, J. P.; Evers, J.; Ilsbroux, J.; Remstedt, H. G.; Somerville, H. J.; H. Van Strien In *Concawe Report*; The Hague, 1984.
(24) Method, P. *Standard Methods for Analysis and Testing of Petroleum and Petroleum Related Products*; Wiley: New York, 1995.
(25) Daghbouche, Y.; Garrigues, S.; MoralesRubio, A.; delaGuardia, M. *Anal. Chim. Acta* **1997**, *345*, 161–171.
(26) Minty, B.; Ramsey, E. D.; Davies, I.; James, D. I.; O'Brien, P. M.; Littlewood, M. I. *Anal. Commun.* **1998**, *35*, 277–280.
(27) Romero, M. T.; Ferrer, N. *Anal. Chim. Acta* **1999**, *395*, 77–84.
(28) Wells, M. J. M.; Ferguson, D. M.; Green, J. C. *Analyst* **1995**, *120*, 1715–1721.
(29) Ramsey, E. D. *J. Supercrit. Fluids* **2008**, *44*, 201–210.
(30) Ramsey, E. D.; Wei, G. *Int. J. Environ. Anal. Chem.* **2008**, *88*, 957–968.
(31) http://www.perkinelmer.com/ (accessed on 10/17/2011).
(32) Noble, D. *Anal. Chem.* **1993**, *65*, A693–A695.
(33) McCrum, W. A.; Whittle, P. J. *Analyst* **1982**, *107*, 1081–1085.
(34) Whittle, P. J.; McCrum, W. A.; Horne, M. W. *Analyst* **1980**, *105*, 679–684.
(35) Heinrich, P.; Wyzgol, R.; Schrader, B.; Hatzilazaru, A.; Luebbers, D. W. *Appl. Spectrosc.* **1990**, *44*, 1641–1646.
(36) Janotta, M.; Karlowatz, M.; Vogt, F.; Mizaikoff, B. *Anal. Chim. Acta* **2003**, *496*, 339–348.
(37) Karlowatz, M.; Kraft, M.; Mizaikoff, B. *Anal. Chem.* **2004**, *76*, 2643–2648.
(38) Dobbs, G. T.; Balu, B.; Young, C.; Kranz, C.; Hess, D. W.; Mizaikoff, B. *Anal. Chem.* **2007**, *79*, 9566–9571.
(39) Kurusu, Y.; Masuyama, Y.; Yanagi, K.; Morinaga, H.; Yamamoto, S.; Makanishi, M. *Bull. Chem. Soc. Jpn.* **1993**, *66*, 673–675.
(40) Ouyang, Y.; Mansell, R. S.; Rhue, R. D. *Ground Water* **1995**, *33*, 399–406.
(41) Sprow, F. B. *AIChe J.* **1967**, *13*, 995–998.
(42) Peralta-Martinez, M. V.; Arriola-Medellin, A.; Manzanares-Papayanopoulos, E.; Sanchez-Sanchez, R.; Palacios-Lozano, E. M. *Pet. Sci. Technol.* **2004**, *22*, 1035–1043.
(43) Ramirez, M.; Bullon, J.; Anderez, J.; Mira, I.; Salager, J. L. *J. Dispersion Sci. Technol.* **2002**, *23*, 309–321.
(44) Mlynek, Y.; Resnick, W. *AIChe J.* **1972**, *18*, 122–127.
(45) Marechal, Y. *J. Chem. Phys.* **1991**, *95*, 5565–5573.
(46) Atkins, P.; de Paula, J. *Physical Chemistry*, 7th ed.; W.H. Freeman: New York, 2002.
(47) Luzinov, I.; Xi, K.; Pagnoulle, C.; Huynh-Ba, G.; Jerome, R. *Polymer* **1999**, *40*, 2511–2520.
(48) Sperling, L. H. *Polymeric Multicomponent Materials*; Wiley-Interscience: New York, 1998.
(49) Jung, Y. C.; Bhushan, B. *Langmuir* **2009**, *25*, 14165–14173.
(50) Hobbs, S. Y.; Dekkers, M. E. J.; Watkins, V. H. *Polymer* **1988**, *29*, 1598–1602.
(51) Van Krevelen, D. W. *Properties of Polymers*, 3rd ed.; Elsevier: Amsterdam, 1997.
(52) Zdyrko, B.; Iyer, K. S.; Luzinov, I. *Polymer* **2006**, *47*, 272–279.
(53) Cambiella, A.; Benito, J. M.; Pazos, C.; Coca, J.; Ratoi, M.; Spikes, H. A. *Tribol. Lett.* **2006**, *22*, 53–65.
(54) Janczuk, B.; Wojcik, W.; Zdziennicka, A.; Bruque, J. M. *Powder Technol.* **1996**, *86*, 229–238.